PERGAMON

International Journal of Heat and Mass Transfer 45 (2002) 3651–3665

International Journal of HEAT and MASS TRANSFER

www.elsevier.com/locate/ijhmt

Average momentum equation for interdendritic flow in a solidifying columnar mushy zone

P. Bousquet-Melou [a], B. Goyeau [b,*], M. Quintard [c], F. Fichot [a], D. Gobin [b]

[a] *Institut de Protection et de Sûreté Nucléaire, C.E.A Cadarache, Bât. 700, 13108 Saint Paul Lez Durance, France*

[b] *Laboratoire FAST, Universités Paris VI et Paris XI, UMR CNRS 7608, Bât. 502, Campus Universitaire, 91405 Orsay Cedex, France*

[c] *Institut de Mécanique des Fluides de Toulouse, Avenue du Professeur Camille Soula, 31400 Toulouse, France*

Received 20 November 2001

Abstract

This paper deals with the derivation of the macroscopic momentum transport equation in a *non-homogeneous solidifying columnar dendritic* mushy zone using the method of volume averaging. One of the originalities of this study lies in the derivation of an associated *closure problem* for the determination of the spatial evolution of the effective transport properties in such a complex situation. In this analysis – where the phase change has been included at the different stages of the derivation – all the terms arising from the averaging procedure (geometrical moments, phase interactions, interfacial momentum transport due to phase change, porosity gradients, etc.) are systematically estimated and compared on the basis of the characteristic length-scale constraints associated with the porous structures presenting *evolving heterogeneities*. For dendritic structures with "moderate" (but not small) evolving heterogeneities, we show that phase change and non local effects could hardly affect the determination of the permeability and inertia tensors. Finally, a closed form of the macroscopic momentum equation is proposed and a discussion is presented about the need to consider inertia terms and the second Brinkman correction (explicitly involving gradients of the liquid volume fraction) in such non-homogeneous systems.

1. Introduction

Fluid mechanics in a multi-component mixture during solidification is a very complex problem due to the development of a two-phase columnar mushy zone. This mushy zone is composed of solid dendrites and interdendritic liquid (Fig. 1) and its evolution depends on several conditions such as temperature gradient, initial concentration of the melt, cooling rate, etc. It is now recognized as essential to give the most possible accurate description of transport phenomena in the mushy zone since the interdendritic liquid flow, mainly induced by thermosolutal natural convection [1], strongly influences heat and mass transfer, and plays a key role on the micro- and macro-segregation [2]. Under these circumstances, the solidification rate, the microstructure and the quality of the product (homogeneity, reliability, aspect, etc.) can be drastically affected.

In most solidification models, the mushy zone is described as a porous medium (or equivalent continuum) and the momentum equation has been derived using different methods reviewed in detail by [3]. Two distinct approaches have been used to represent the coupling between the mushy and bulk liquid regions. In the *multi-domain* approach, the Navier–Stokes equation is written in the fully melted region while the flow in the porous mushy layer is governed by Darcy's law or one of its extensions, and appropriate boundary conditions are written at the interface [4–6]. However, this two-domain method is not suitable for predicting irregular interface shapes and, furthermore, interfacial boundary conditions still remain a controversial subject of intense research activity [7]. For these reasons, multi-domain models have been replaced by the more convenient *one-domain* continuum model constituted of a single set of equations describing the transport phenomena in the

* Corresponding author. Tel.: +33-1-69-15-80-39.
E-mail address: goyeau@fast.u-psud.fr (B. Goyeau).

0017-9310/02/$ - see front matter
PII: S0017-9310(02)00077-7

Nomenclature

$\mathbf{A}_{\beta e}$	area of entrances and exits for the β-phase contained within the averaging volume, m^2
$\mathbf{A}_{\beta\sigma}$	β–σ interface contained within the averaging volume, m^2
A_v	specific area, m^{-1}
$\mathbf{b}$	vector used to represent $\widetilde{P}_\beta$ when microscopic inertial effects are negligible, m^{-1}
$\mathbf{B}$	second-order tensor used to represent $\widetilde{\mathbf{w}}_{\beta\sigma}$ when microscopic inertial effects are negligible
$\mathbf{c}$	vector used to represent the contribution of microscopic inertial effects to $\widetilde{P}_\beta$, m^{-1}
$\mathbf{C}$	second-order tensor used to represent the contribution of microscopic inertial effects to $\widetilde{\mathbf{w}}_{\beta\sigma}$
$\mathbf{F}$	inertia tensor
$\mathbf{g}$	gravitational acceleration, m s^{-2}
$\mathbf{K}$	permeability tensor, m^2
ℓ_i	$i = 1, 2, 3$, lattice vectors, m
ℓ_β	interdendritic length scale, m
L	characteristic length for macroscopic quantities, m
L_v	characteristic length for $\langle \mathbf{v}_\beta \rangle^\beta$, m
L_ε	characteristic length for ε_β, m
$\mathbf{m}$	vector used to represent $\widetilde{P}_\beta$, m^{-1}
$\dot{m}_\beta$	melting rate, kg m^{-3} s^{-1}
$\dot{m}_\sigma$	solidification rate, kg m^{-3} s^{-1}
$\mathbf{M}$	second-order tensor used to represent $\widetilde{\mathbf{v}}_\beta$
$\mathbf{n}_{\beta\sigma}$	unit normal vector directed from the β-phase toward the σ-phase
P_β	pression in the β-phase, Pa
$\mathbf{r}$	position vector, m
r_0	radius of the averaging volume, m
t	time, s
$\widetilde{t}$	time scale for $\widetilde{\mathbf{v}}_\beta$, s
t^*	time scale for $\langle \mathbf{v}_\beta \rangle^\beta$, s
$\mathbf{t}_{\beta\sigma}$	unit tangent vector at the β–σ interface
$\mathbf{v}_\beta$	velocity of the β-phase, m s^{-1}
V	averaging volume, m^3
V_β	volume of the β-phase contained within the averaging volume, m^3
$\mathbf{w}_{\beta\sigma}$	velocity of the β–σ interface, m s^{-1}
$\overline{w}_n$	averaged growth velocity, m s^{-1}
$\mathbf{x}$	position of the centroid of the averaging volume, m
$\mathbf{y}$	position vector relative to the centroid of the averaging volume, m

Greek symbols

δ	$1 - \rho_\sigma/\rho_\beta$, shrinkage parameter
γ_β	indicator function for the β-phase
ε_β	volume fraction of the β-phase
μ_β	dynamic viscosity of the β-phase, Pa s
ρ_β	density of the β-phase, kg m^{-3}
$\langle \psi_\beta \rangle$	superficial volume average of ψ in the β-phase
$\langle \psi_\beta \rangle^\beta$	intrinsic phase average of ψ in the β-phase
$\widetilde{\psi}_\beta$	spatial fluctuation of ψ in the β-phase

Subscripts

β	liquid phase
σ	solid phase

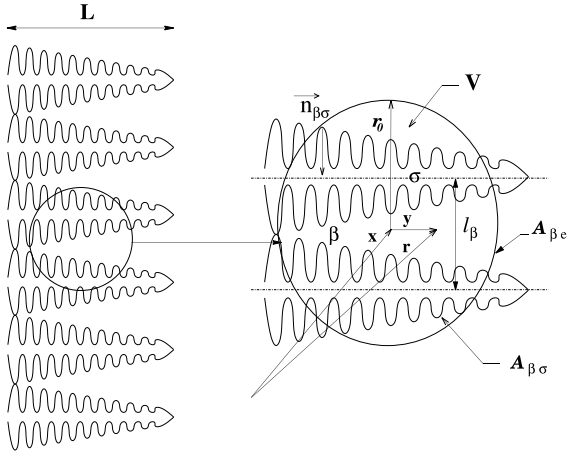

Fig. 1. Macroscopic dendritic mushy zone and an associated averaging volume.

whole domain (melt, mush and solid regions). In this approach, quasi-steady approximations, remeshing or coordinate mapping are not necessary anymore, and the conservation equations can be numerically solved using a fixed grid.

Two kinds of continuum models have been used to derive the conservation equations in the context of solidification: the classical *mixture theory* [8–10] and the *volume averaging method* [11–13]. The former treats the solid and liquid phases as a solid–liquid mixture to which macroscopic properties are assigned in a purely phenomenological manner. Conservation equations for each phase are added to provide a set of mixture conservation equations and interactions between phases are described using semi-empirical relationships. One of the first complete solidification models for multi-component systems using the mixture theory has been developed by Bennon and Incropera [9] and later reassessed by Prescott et al. [10]. This mathematical model has been ex-

tended by some authors [14–16] and have been extensively used in numerous configurations [17–21].

The volume averaging technique considers a representative elementary volume in the domain under study, and the local conservation equations are integrated over this volume providing averaged *macroscopic* transport equations valid in the whole domain [22,23]. Phase interactions at the solid–liquid interface arise from the averaging process and are represented by interfacial area integrals. This technique has been used first in solidification modeling by Beckermann and Viskanta [24] and later extended and used by Ganesan and Poirier [11], Ni and Beckermann [12], Beckermann and Viskanta [25] and Schneider and Beckermann [26]. Due to the complexity of the dendritic structures, phase interaction integral terms are not explicitly calculated in these models and generally are also represented by semi-empirical laws. Recently, a multiphase/multiscale theory has provided some progress in this issue, by describing finite mass exchange in the solid and extradendritic liquid in an averaging volume [27]. The method of volume averaging is often preferred due to its ability to include microscopic information at the macroscopic scale thus improving solidification modeling.

Regarding the momentum equation, Prescott et al. [10] have shown that under the same physical assumptions, continuum and volume-averaged approaches give rise to equivalent macroscopic equations to describe the interdendritic flow. Indeed, in both cases, the macroscopic momentum conservation equation is represented by a modified Navier–Stokes equation including Darcy's term sometimes completed with a Forchheimer correction term where porosity and the permeability are generally related by the classical Kozeny–Carman relationship. Let us note that, *in the absence of phase change*, the derivation of Darcy's law for homogeneous systems has also been obtained using the homogenization theory [28,29].

All comparisons between numerical simulations and experiments were found in qualitative agreement, but important discrepancies still subsist between measured and predicted fields [19,24,30,31]. These differences are mainly attributed to the weakness of the model assumptions, such as local thermal and mass equilibria, uncertainty on physical properties and geometrical characterization of the columnar dendritic mushy zone. It is henceforth clear that one significant improvement in solidification modeling lies in the introduction of microscopic information both in the macroscopic conservation equations and in the representation of the effective transport coefficients such as permeability, diffusion–dispersion coefficient or effective conductivity.

Among the limitations of the previous derivations of the macroscopic momentum equation used in solidification modeling, we note that dispersive fluxes and inertial effects are generally intuitively neglected and, as previously emphasized, phase interaction terms are estimated by constitutive laws. Furthermore, besides its strong anisotropy, the dendritic columnar region is characterized by non-uniformity of the macroscopic properties such as the liquid volume fraction which *continuously* varies from zero in the solid to unity in the melt region. Although these *continuous variations* or *evolving heterogeneities* [32] can obviously modify the convective flows [33], they have been rarely *explicitly* included in the theoretical models. Finally, one of the most important limitation of interdendritic flow modelization comes from the Kozeny–Carman relationship used to estimate the permeability from the liquid volume fraction. Several numerical and experimental attempts have been made to provide a better representation of the permeability, especially for liquid volume fractions greater than 0.7 [34–37] but more data are still necessary to provide a general description.

In order to overcome the above limitations, this paper addresses a new derivation of the macroscopic momentum equation in a solidifying columnar dendritic mushy zone using the volume averaging method and provides an associated *closure problem* for the characterization of the spatial evolution of the transport properties in such heterogeneous structures. The concept of closure problem has been previously used in homogeneous [38–40] or heterogeneous [37] porous media but always *in the absence of phase change*. In the context of solidification, the analysis becomes much more complex and a full solution taking into account all the phenomena at the different scales is still out of reach. For this reason, in order to *quantitatively* justify the necessary simplifications and to propose a closed form of the macroscopic momentum equation, all the micro- and macro-contributions to momentum transport due to phase change and geometry are estimated and compared on the basis of the characteristic length-scale constraints associated with the dendritic-like porous structures presenting *evolving heterogeneities*.

2. The procedure of volume averaging

In order to derive the macroscopic momentum equations for an incompressible flow of a binary mixture during solidification, we consider a *columnar mushy zone* and the local averaging volume V shown in Fig. 1, where r_0 is the radius of V and ℓ_β stands for the interdendritic characteristic length. All physical properties of the mixture are assumed to be constant and the Boussinesq approximation applies. The boundary-value problem describing the mass and momentum conservation within the averaging volume is given by:

$$\frac{\partial \rho_\beta}{\partial t} + \nabla \cdot (\rho_\beta \mathbf{v}_\beta) = 0 \tag{1}$$

$$\frac{\partial}{\partial t}(\rho_\beta \mathbf{v}_\beta) + \nabla \cdot (\rho_\beta \mathbf{v}_\beta \mathbf{v}_\beta) = -\nabla P_\beta + \mu_\beta \nabla^2 \mathbf{v}_\beta + \rho_\beta \mathbf{g} \quad \text{in the } \beta\text{-phase} \tag{2}$$

$$\rho_\beta \mathbf{n}_{\beta\sigma} \cdot (\mathbf{v}_\beta - \mathbf{w}_{\beta\sigma}) = \rho_\sigma \mathbf{n}_{\beta\sigma} \cdot (\mathbf{v}_\sigma - \mathbf{w}_{\beta\sigma}) \quad \text{at } \mathbf{A}_{\beta\sigma}, \tag{3}$$

$$\mathbf{v}_\beta = f(\mathbf{r}, t) \quad \text{at } \mathbf{A}_{\beta e}, \tag{4}$$

where the boundary condition (3) represents the mass conservation equation at the solid–liquid interface $\mathbf{A}_{\beta\sigma}$, and $\mathbf{A}_{\beta e}$ in (4) is the area of entrances and exits of the liquid phase in the macroscopic region V (Fig. 1). At this stage, this boundary condition is unknown and the discussion about the function $f(\mathbf{r}, t)$ will take place in the section about the closure problem. It should be emphasized here that the physical situation we want to deal with can be much more complicated than the problem considered in this section. In particular, mass conservation of several species, and heat transfer could be considered. However, the relaxation times associated with these other mechanisms are in most situations much larger than the relaxation time associated with the viscous flow under consideration. Therefore, we will neglect the possible coupling between the momentum balance and these other transport mechanisms.

2.1. Geometrical considerations

In homogeneous structures, one usually consider that the averaging method is applicable for systems in which the different length scales are constrained by [22,23]:

$$\ell_\beta \ll r_0 \ll L, \tag{5}$$

where L is the macroscopic length scale of the system. For a columnar dendritic-like porous structure presenting evolving heterogeneities the situation is much more complex since the averaged macroscopic properties are space-dependent but also depend on the size of the averaging volume V. Indeed, in a mushy zone, the liquid volume fraction (porosity) continuously varies from unity in the melt to zero in the solid region. In this case, the analysis depends on three length-scale constraints which are functions of some geometrical parameter characteristic of the evolving heterogeneity. This parameter describing the *decreasing rate of the geometry*, denoted τ, will be defined as the average decrease of the thickness of the dendrite in the direction parallel to the primary dendritic arm [32]. First, when the evolving heterogeneities are small (typically $\tau < 0.5\%$), the macroscopic properties are quasi-constant whatever the size r_0 of the averaging volume V and the scale separation is represented by the classical constraint

$$\ell_\beta \ll r_0 \ll L_\varepsilon, \tag{6}$$

where L_ε is the characteristic length associated with the macroscopic variations of porosity. For a "moderate" value of τ (less than 4%), L_ε is not strongly greater than r_0 but the scales still remain distinct and the associated length-scale constraint can be written

$$\ell_\beta < r_0 < L_\varepsilon, \tag{7}$$

which also leads to

$$\ell_\beta \ll L_\varepsilon. \tag{8}$$

Under this condition, the averaging procedure can still be used and we will see in the next section that Eq. (8) is very useful for comparing of the order of magnitude of the different terms during the averaging procedure. Finally, when evolving heterogeneities are important (greater than 4%), scale separation is not respected and a fixed averaging volume may not be adapted to provide average properties. This situation still remains a challenge and an alternative theory could consist in the use of deforming averaging volume [41].

According to the estimation by Goyeau [37] the decreasing rate of the geometry τ for real dendritic structures observed experimentally during solidification of a 26 wt% solution of aqueous NH_4Cl [42] and succinonitrile–4 wt% acetone [43] is less than 4%. Therefore, we will consider in this work columnar dendritic structures with "moderate" value of τ where the scale separation is described by Eqs. (7) and (8).

2.2. Averaged continuity equation

The definitions and theorems used in the following development are summarized in Appendix A. Let us consider the microscopic continuity equation of the solid and liquid phases in the averaging volume V:

$$\frac{\partial \rho_k}{\partial t} + \nabla \cdot (\rho_k \mathbf{v}_k) = 0, \quad k = \beta, \sigma. \tag{9}$$

According to Prescott and Incropera [11] and Ganesan and Poirier [12], we assume that, in the context of solidification, the solid and liquid microscopic densities ρ_σ and ρ_β are uniform in V and that the solid and the liquid density variations are only significant on the macroscopic scale. This assumption can be written:

$$\rho_k = \gamma_k \langle \rho_k \rangle^k, \quad k = \beta, \sigma, \tag{10}$$

where γ_k is the k-phase indicator function, given by definition (A.6). $\langle \rho_k \rangle^k$ represents the intrinsic volume average density of phase k defined by Eq. (A.9). Using the averaging theorems provided in Appendix A, the averaged macroscopic mass conservation equations for the liquid and solid phases can be written as

$$\frac{\partial}{\partial t}(\varepsilon_\beta \rho_\beta) + \nabla \cdot (\varepsilon_\beta \rho_\beta \langle \mathbf{v}_\beta \rangle^\beta) = \dot{\boldsymbol{m}}_\beta, \tag{11}$$

$$\frac{\partial}{\partial t}(\varepsilon_\sigma \rho_\sigma) + \nabla \cdot (\varepsilon_\sigma \rho_\sigma \langle \mathbf{v}_\sigma \rangle^\sigma) = \dot{m}_\sigma, \tag{12}$$

where $\dot{m}_\beta$ and $\dot{m}_\sigma$ are, respectively, the melting and solidification rates defined by:

$$\dot{m}_\beta = -\frac{1}{V}\int_{A_{\beta\sigma}} \rho_\beta \mathbf{n}_{\beta\sigma} \cdot (\mathbf{v}_\beta - \mathbf{w}_{\beta\sigma})\,\mathrm{d}A, \tag{13}$$

$$\dot{m}_\sigma = -\frac{1}{V}\int_{A_{\beta\sigma}} \rho_\sigma \mathbf{n}_{\sigma\beta} \cdot (\mathbf{v}_\sigma - \mathbf{w}_{\beta\sigma})\,\mathrm{d}A, \tag{14}$$

where $\mathbf{w}_{\beta\sigma}$ is the velocity of the interface $\mathbf{A}_{\beta\sigma}$ and $\mathbf{n}_{\beta\sigma}$ is the unit normal vector pointing from the β-phase to the σ-phase. The microscopic mass balance at the solid–liquid interface given by Eq. (3) gives rise to the macroscopic mass balance

$$\dot{m}_\beta + \dot{m}_\sigma = 0. \tag{15}$$

In a columnar mushy zone and in the absence of solid transport, the local solid velocity $\mathbf{v}_\sigma$ due to dilatation is very small compared to the interface velocity $\mathbf{w}_{\beta\sigma}$ and is neglected in this analysis. Therefore, Eq. (3) reduces to

$$\mathbf{n}_{\beta\sigma} \cdot \mathbf{v}_\beta = \delta \mathbf{n}_{\beta\sigma} \cdot \mathbf{w}_{\beta\sigma} \quad \text{at } \mathbf{A}_{\beta\sigma}, \tag{16}$$

where δ is the volume change parameter, defined by:

$$\delta = 1 - \frac{\rho_\sigma}{\rho_\beta}. \tag{17}$$

Using Eqs. (11), (12) and (15) leads to the averaged mass conservation equation for the mixture

$$\frac{\partial}{\partial t}(\varepsilon_\beta \rho_\beta + \varepsilon_\sigma \rho_\sigma) + \nabla \cdot (\varepsilon_\beta \rho_\beta \langle \mathbf{v}_\beta \rangle^\beta) = 0. \tag{18}$$

2.3. Averaged momentum equation

In order to derive the macroscopic momentum equation for the liquid phase, we consider the superficial average of the Navier–Stokes equation (2):

$$\left\langle \frac{\partial}{\partial t}(\rho_\beta \mathbf{v}_\beta) \right\rangle + \left\langle \nabla \cdot (\rho_\beta \mathbf{v}_\beta \mathbf{v}_\beta) \right\rangle = -\left\langle \nabla P_\beta \right\rangle + \left\langle \mu_\beta \nabla^2 \mathbf{v}_\beta \right\rangle + \left\langle \rho_\beta \mathbf{g} \right\rangle. \tag{19}$$

Using Eq. (10) and the derivatives theorems (A.14) and (A.15), each term of Eq. (19) can be developed. Let us start with the left-hand side of Eq. (19):

Averaged accumulation term:

$$\left\langle \frac{\partial}{\partial t}(\rho_\beta \mathbf{v}_\beta) \right\rangle = \frac{\partial}{\partial t}(\varepsilon_\beta \rho_\beta \langle \mathbf{v}_\beta \rangle^\beta) - \frac{1}{V}\int_{A_{\beta\sigma}} (\mathbf{n}_{\beta\sigma} \cdot \mathbf{w}_{\beta\sigma}) \rho_\beta \mathbf{v}_\beta \,\mathrm{d}A. \tag{20}$$

Averaged convective term:

$$\left\langle \nabla \cdot (\rho_\beta \mathbf{v}_\beta \mathbf{v}_\beta) \right\rangle = \nabla \cdot (\varepsilon_\beta \rho_\beta \langle \mathbf{v}_\beta \mathbf{v}_\beta \rangle^\beta) + \frac{1}{V}\int_{A_{\beta\sigma}} (\mathbf{n}_{\beta\sigma} \cdot \mathbf{v}_\beta) \rho_\beta \mathbf{v}_\beta \,\mathrm{d}A. \tag{21}$$

Using the Gray decomposition [44]:

$$\mathbf{v}_\beta = \langle \mathbf{v}_\beta \rangle^\beta + \widetilde{\mathbf{v}}_\beta, \tag{22}$$

where $\widetilde{\mathbf{v}}_\beta$ is the spatial velocity deviation, allows to write the term $\langle \mathbf{v}_\beta \mathbf{v}_\beta \rangle^\beta$ of Eq. (21) under the simplified form

$$\langle \mathbf{v}_\beta \mathbf{v}_\beta \rangle^\beta = \langle \mathbf{v}_\beta \rangle^\beta \langle \mathbf{v}_\beta \rangle^\beta + \langle \widetilde{\mathbf{v}}_\beta \widetilde{\mathbf{v}}_\beta \rangle^\beta, \tag{23}$$

where $\langle \widetilde{\mathbf{v}}_\beta \widetilde{\mathbf{v}}_\beta \rangle^\beta$ is the liquid momentum dispersion. The simplified form (23) requires that the different length scales verify [45]

$$\left(\frac{r_0}{L}\right)^2 \ll \frac{l_\beta}{L}. \tag{24}$$

The above condition resulting from Eq. (5) is always satisfied for homogeneous porous media. This is not the case for columnar dendritic porous structures presenting evolving heterogeneities, where scale separation depends on the decreasing rate of the geometry τ. Using schematic dendritic structures Benihaddadene [13] has shown that (24) is verified only for very small values of τ ($\tau \sim 0.5\%$) and that for "moderate" values of τ (less than 4%), Eq. (24) becomes

$$\left(\frac{r_0}{L}\right)^2 < \frac{l_\beta}{L}. \tag{25}$$

Under these circumstances, Eq. (23) remains valid and the left-hand side of Eq. (19) becomes

$$\left\langle \frac{\partial}{\partial t}(\rho_\beta \mathbf{v}_\beta) \right\rangle + \left\langle \nabla \cdot (\rho_\beta \mathbf{v}_\beta \mathbf{v}_\beta) \right\rangle = \frac{\partial}{\partial t}(\varepsilon_\beta \rho_\beta \langle \mathbf{v}_\beta \rangle^\beta) + \nabla \cdot (\varepsilon_\beta \rho_\beta \langle \mathbf{v}_\beta \rangle^\beta \langle \mathbf{v}_\beta \rangle^\beta) + \nabla \cdot (\varepsilon_\beta \rho_\beta \langle \widetilde{\mathbf{v}}_\beta \widetilde{\mathbf{v}}_\beta \rangle^\beta) + \frac{1}{V}\int_{A_{\beta\sigma}} \mathbf{n}_{\beta\sigma} \cdot (\mathbf{v}_\beta - \mathbf{w}_{\beta\sigma}) \rho_\beta \mathbf{v}_\beta \,\mathrm{d}A. \tag{26}$$

Let us consider now the right-hand side of Eq. (19):

Averaged pressure term:

$$\left\langle -\nabla P_\beta \right\rangle = -\nabla(\varepsilon_\beta \langle P_\beta \rangle^\beta) - \frac{1}{V}\int_{A_{\beta\sigma}} \mathbf{n}_{\beta\sigma} P_\beta \,\mathrm{d}A. \tag{27}$$

If we use the Gray decomposition for pressure in the last term of Eq. (27), the area integral can be written:

$$\frac{1}{V}\int_{A_{\beta\sigma}} \mathbf{n}_{\beta\sigma} P_\beta|_{\mathbf{r}}\,\mathrm{d}A = \frac{1}{V}\int_{A_{\beta\sigma}} \mathbf{n}_{\beta\sigma} \langle P_\beta \rangle^\beta|_{\mathbf{r}}\,\mathrm{d}A + \frac{1}{V}\int_{A_{\beta\sigma}} \mathbf{n}_{\beta\sigma} \widetilde{P}_\beta|_{\mathbf{r}}\,\mathrm{d}A. \tag{28}$$

Here, we are confronted to the fact that the first area integral in the right-hand side of Eq. (28) contains the

average quantity $\langle P_\beta\rangle^\beta|_{\mathbf{r}}$ which is evaluated at $\mathbf{r}$ instead of the centroid $\mathbf{x}$ of the averaging volume (Fig. 1). According to Quintard and Whitaker [46], we can overcome this difficulty using Taylor series expansions of this quantity about the centroid $\mathbf{x}$ of the averaging volume

$$\langle P_\beta\rangle^\beta|_{\mathbf{r}} = \langle P_\beta\rangle^\beta|_{\mathbf{x}} + \mathbf{y}\cdot\nabla\langle P_\beta\rangle^\beta|_{\mathbf{x}} + \frac{1}{2}\mathbf{yy}:\nabla\nabla\langle P_\beta\rangle^\beta|_{\mathbf{x}} + \cdots \tag{29}$$

where $\mathbf{y} = \mathbf{r} - \mathbf{x}$. Substitution of expression (29) in (28) yields

$$\begin{aligned}\frac{1}{V}\int_{A_{\beta\sigma}} \mathbf{n}_{\beta\sigma}\langle P_\beta\rangle^\beta|_{\mathbf{r}}\,\mathrm{d}A &= \left(\frac{1}{V}\int_{A_{\beta\sigma}}\mathbf{n}_{\beta\sigma}\,\mathrm{d}A\right)\langle P_\beta\rangle^\beta|_{\mathbf{x}} + \left(\frac{1}{V}\int_{A_{\beta\sigma}}\mathbf{n}_{\beta\sigma}\mathbf{y}\,\mathrm{d}A\right)\\ &\quad\cdot\nabla\langle P_\beta\rangle^\beta|_{\mathbf{x}} + \frac{1}{2}\left(\frac{1}{V}\int_{A_{\beta\sigma}}\mathbf{n}_{\beta\sigma}\mathbf{yy}\,\mathrm{d}A\right):\nabla\nabla\langle P_\beta\rangle^\beta|_{\mathbf{x}}\\ &\quad+\cdots\end{aligned} \tag{30}$$

Using schematic and real dendritic structures, it may be shown [32,37] that the geometrical moments of Eq. (30)

$$\frac{1}{V}\int_{A_{\beta\sigma}}\mathbf{n}_{\beta\sigma}\mathbf{y}\,\mathrm{d}A,\quad \frac{1}{V}\int_{A_{\beta\sigma}}\mathbf{n}_{\beta\sigma}\mathbf{yy}\,\mathrm{d}A,\ldots \tag{31}$$

are very small compared to unity and therefore can be neglected in the analysis. Furthermore, using the averaging theorem (A.14) with $\psi_\beta = \gamma_\beta$ leads to

$$\frac{1}{V}\int_{A_{\beta\sigma}}\mathbf{n}_{\beta\sigma}\,\mathrm{d}A = -\nabla\varepsilon_\beta \tag{32}$$

and expression (30) becomes

$$\frac{1}{V}\int_{A_{\beta\sigma}}\mathbf{n}_{\beta\sigma}\langle P_\beta\rangle^\beta|_{\mathbf{r}}\,\mathrm{d}A \simeq -\nabla\varepsilon_\beta\langle P_\beta\rangle^\beta|_{\mathbf{x}} = -\nabla\varepsilon_\beta\langle P_\beta\rangle^\beta. \tag{33}$$

Finally the averaged pressure term takes the form:

$$\langle -\nabla P_\beta\rangle = -\varepsilon_\beta\nabla\langle P_\beta\rangle^\beta - \frac{1}{V}\int_{A_{\beta\sigma}}\mathbf{n}_{\beta\sigma}\widetilde{P}_\beta\,\mathrm{d}A. \tag{34}$$

Averaged viscous term:

If the liquid viscosity is assumed to be constant, the averaged viscous term is given by

$$\begin{aligned}\langle\mu_\beta\nabla^2\mathbf{v}_\beta\rangle &= \mu_\beta\nabla^2\cdot(\varepsilon_\beta\langle\mathbf{v}_\beta\rangle^\beta)\\ &\quad+\mu_\beta\nabla\cdot\left(\frac{1}{V}\int_{A_{\beta\sigma}}\mathbf{n}_{\beta\sigma}\mathbf{v}_\beta\,\mathrm{d}A\right)\\ &\quad+\frac{\mu_\beta}{V}\int_{A_{\beta\sigma}}\mathbf{n}_{\beta\sigma}\cdot\nabla\mathbf{v}_\beta\,\mathrm{d}A.\end{aligned} \tag{35}$$

Using the Gray velocity decomposition (22) in the last area integral of Eq. (35) provides

$$\begin{aligned}\frac{\mu_\beta}{V}\int_{A_{\beta\sigma}}\mathbf{n}_{\beta\sigma}\cdot\nabla\mathbf{v}_\beta|_{\mathbf{r}}\,\mathrm{d}A &= \frac{\mu_\beta}{V}\int_{A_{\beta\sigma}}\mathbf{n}_{\beta\sigma}\cdot\nabla\langle\mathbf{v}_\beta\rangle^\beta|_{\mathbf{r}}\,\mathrm{d}A\\ &\quad+\frac{\mu_\beta}{V}\int_{A_{\beta\sigma}}\mathbf{n}_{\beta\sigma}\cdot\nabla\widetilde{\mathbf{v}}_\beta|_{\mathbf{r}}\,\mathrm{d}A,\end{aligned} \tag{36}$$

where the $\langle\mathbf{v}_\beta\rangle^\beta|_{\mathbf{r}}$ in the first area integral of Eq. (36) has to be developed into Taylor series expansions about the centroid $\mathbf{x}$ of the averaging volume. Since geometrical terms (31) are negligible this integral takes the form

$$\frac{\mu_\beta}{V}\int_{A_{\beta\sigma}}\mathbf{n}_{\beta\sigma}\cdot\nabla\langle\mathbf{v}_\beta\rangle^\beta|_{\mathbf{r}}\,\mathrm{d}A \simeq -\mu_\beta\nabla\varepsilon_\beta\cdot\nabla\langle\mathbf{v}_\beta\rangle^\beta|_{\mathbf{x}}. \tag{37}$$

Therefore, using (36) and (37) in (35) gives rise to

$$\begin{aligned}\langle\mu_\beta\nabla^2\mathbf{v}_\beta\rangle &= \varepsilon_\beta\mu_\beta\nabla^2\langle\mathbf{v}_\beta\rangle^\beta + \mu_\beta\nabla\varepsilon_\beta\cdot\nabla\langle\mathbf{v}_\beta\rangle^\beta\\ &\quad+\mu_\beta\nabla^2\varepsilon_\beta\langle\mathbf{v}_\beta\rangle^\beta + \frac{\mu_\beta}{V}\int_{A_{\beta\sigma}}\mathbf{n}_{\beta\sigma}\cdot\nabla\widetilde{\mathbf{v}}_\beta\,\mathrm{d}A\\ &\quad+\mu_\beta\nabla\cdot\left[\frac{1}{V}\int_{A_{\beta\sigma}}\mathbf{n}_{\beta\sigma}\mathbf{v}_\beta\,\mathrm{d}A\right].\end{aligned} \tag{38}$$

In the absence of phase change, the last area integral of (38) vanishes due to the no-slip and no-penetration conditions ($\mathbf{v}_\beta = 0$) at the solid–liquid interface and the average of the viscous term (38) takes the classical form derived in [32].

Since we are dealing with a phase change problem, according to the mass conservation Eq. (16), the liquid velocity is a priori not zero at the solid–liquid interface, due to the volume change ($\delta \neq 0$) upon solidification. If we use again Gray's decomposition in the last area integral of (38), we obtain

$$\begin{aligned}&\nabla\cdot\left[\frac{1}{V}\int_{A_{\beta\sigma}}\mathbf{n}_{\beta\sigma}\mathbf{v}_\beta|_{\mathbf{r}}\,\mathrm{d}A\right]\\ &\quad=\nabla\cdot\left[\frac{1}{V}\int_{A_{\beta\sigma}}\mathbf{n}_{\beta\sigma}\langle\mathbf{v}_\beta\rangle^\beta|_{\mathbf{r}}\,\mathrm{d}A\right]\\ &\qquad+\nabla\cdot\left[\frac{1}{V}\int_{A_{\beta\sigma}}\mathbf{n}_{\beta\sigma}\widetilde{\mathbf{v}}_\beta|_{\mathbf{r}}\,\mathrm{d}A\right]\end{aligned} \tag{39}$$

and as previously, it is easy to show that

$$\nabla\cdot\left[\frac{1}{V}\int_{A_{\beta\sigma}}\mathbf{n}_{\beta\sigma}\langle\mathbf{v}_\beta\rangle^\beta|_{\mathbf{r}}\,\mathrm{d}A\right] \simeq -\nabla\varepsilon_\beta\langle\mathbf{v}_\beta\rangle^\beta|_{\mathbf{x}}. \tag{40}$$

Finally, the macroscopic viscous term can be written under the simplified form:

$$\begin{aligned}\langle\mu_\beta\nabla^2\mathbf{v}_\beta\rangle &= \varepsilon_\beta\mu_\beta\nabla^2\langle\mathbf{v}_\beta\rangle^\beta + \frac{\mu_\beta}{V}\int_{A_{\beta\sigma}}\mathbf{n}_{\beta\sigma}\cdot\nabla\widetilde{\mathbf{v}}_\beta\,\mathrm{d}A\\ &\quad+\mu_\beta\nabla\cdot\left[\frac{1}{V}\int_{A_{\beta\sigma}}\mathbf{n}_{\beta\sigma}\widetilde{\mathbf{v}}_\beta\,\mathrm{d}A\right].\end{aligned} \tag{41}$$

Averaged buoyancy term:

$$\langle \rho_\beta \mathbf{g} \rangle = \varepsilon_\beta \langle \rho_\beta \rangle^\beta \mathbf{g} = \varepsilon_\beta \rho_\beta \mathbf{g}. \tag{42}$$

Finally, the different averaged terms (26), (34), (41) and (42) provide the following non-closed averaged momentum equation for the liquid flow through the mushy zone:

$$\begin{aligned}
&\frac{\partial}{\partial t}(\varepsilon_\beta \rho_\beta \langle \mathbf{v}_\beta \rangle^\beta) + \nabla \cdot (\varepsilon_\beta \rho_\beta \langle \mathbf{v}_\beta \rangle^\beta \langle \mathbf{v}_\beta \rangle^\beta) + \nabla \cdot (\varepsilon_\beta \rho_\beta \langle \widetilde{\mathbf{v}}_\beta \widetilde{\mathbf{v}}_\beta \rangle^\beta) \\
&\quad + \frac{1}{V} \int_{A_{\beta\sigma}} (\mathbf{n}_{\beta\sigma} \cdot (\mathbf{v}_\beta - \mathbf{w}_{\beta\sigma}) \rho_\beta \mathbf{v}_\beta \, \mathrm{d}A \\
&\quad = -\varepsilon_\beta \nabla \langle P_\beta \rangle^\beta + \varepsilon_\beta \mu_\beta \nabla^2 \langle \mathbf{v}_\beta \rangle^\beta + \varepsilon_\beta \rho_\beta \mathbf{g} \\
&\qquad + \frac{1}{V} \int_{A_{\beta\sigma}} \mathbf{n}_{\beta\sigma} \cdot (-\widetilde{P}_\beta \mathbf{I} + \mu_\beta \nabla \widetilde{\mathbf{v}}_\beta) \, \mathrm{d}A \\
&\qquad + \mu_\beta \nabla \cdot \left[\frac{1}{V} \int_{A_{\beta\sigma}} \mathbf{n}_{\beta\sigma} \widetilde{\mathbf{v}}_\beta \, \mathrm{d}A \right].
\end{aligned} \tag{43}$$

In order to develop a closed form of equations (11) and (43), a closure problem has to be written to express $\widetilde{P}_\beta$ and $\widetilde{\mathbf{v}}_\beta$ deviations in terms of the intrinsic averaged pressure and velocity $\langle P_\beta \rangle^\beta$ and $\langle \mathbf{v}_\beta \rangle^\beta$.

3. Closure problem

The derivation of the closure problem is very important since it allows to include microscopic aspects such as the tortuosity of the microstructure or microscopic inertia effects in the macroscopic model. This can obviously contribute to significantly improve the geometrical description of the mushy zone in terms of macroscopic properties and therefore increase the quality of the representation of the physical phenomena in solidification modelling.

3.1. Continuity equation

Using Gray's decomposition (22) in Eq. (1) and subtracting the averaged equation (11) leads to the local continuity equation:

$$\varepsilon_\beta \rho_\beta \nabla \cdot \widetilde{\mathbf{v}}_\beta + \varepsilon_\beta \widetilde{\mathbf{v}}_\beta \cdot \nabla \rho_\beta = \rho_\beta \frac{\partial \varepsilon_\beta}{\partial t} + \rho_\beta \nabla \varepsilon_\beta \cdot \langle \mathbf{v}_\beta \rangle^\beta - \dot{m}_\beta. \tag{44}$$

The associated boundary condition is also obtained using Eq. (22) in (3):

$$\mathbf{n}_{\beta\sigma} \cdot \widetilde{\mathbf{v}}_\beta = \delta \mathbf{n}_{\beta\sigma} \cdot \mathbf{w}_{\beta\sigma} - \mathbf{n}_{\beta\sigma} \cdot \langle \mathbf{v}_\beta \rangle^\beta \quad \text{at } \mathbf{A}_{\beta\sigma}. \tag{45}$$

According to the mass balance equation (16), the liquid velocity at the solid–liquid interface $\mathbf{A}_{\beta\sigma}$ is non-zero during phase change if the density of the two phases are different ($\delta \neq 0$). Indeed, in solidification processes, the interdendritic liquid velocity results from double-diffusive natural convection but also from shrinkage ($\delta < 0$) or expansion ($\delta > 0$). This latter phenomena can contribute to morphological instability [47] and macrosegregation [48]. Volume change can also play a key role on the formation of gas micropores due to strong pressure gradients [1,49,50] and may have a significant influence on the velocity field at high solidification rates [3] or in microgravity systems [51].

However, volume expansion or contraction generally hardly influences the interdendritic flow when the volume-change parameter δ is small, which is the case for most metal alloys where $|\delta| \leqslant 10\%$. Furthermore, if we consider that, in most solidification processes, the growth velocity $\mathbf{n}_{\beta\sigma} \cdot \mathbf{w}_{\beta\sigma}$ is small compared to the averaged liquid velocity $\langle \mathbf{v}_\beta \rangle^\beta$ induced by natural convection we can estimate from Eq. (45) that

$$|\delta \mathbf{n}_{\beta\sigma} \cdot \mathbf{w}_{\beta\sigma}| \ll |\mathbf{n}_{\beta\sigma} \cdot \langle \mathbf{v}_\beta \rangle^\beta|. \tag{46}$$

Therefore, the boundary condition (45) reduces to

$$\mathbf{n}_{\beta\sigma} \cdot \widetilde{\mathbf{v}}_\beta = -\mathbf{n}_{\beta\sigma} \cdot \langle \mathbf{v}_\beta \rangle^\beta \quad \text{at } \mathbf{A}_{\beta\sigma}. \tag{47}$$

Moreover, the no-slip boundary condition is given by

$$\vec{\Pi}(\mathbf{v}_\beta) = \vec{\Pi}(\mathbf{v}_\sigma) \quad \text{at } \mathbf{A}_{\beta\sigma}, \tag{48}$$

where $\vec{\Pi}(\cdot)$ is a projection operator on the tangent plane to the interface. Since $\mathbf{v}_\sigma = 0$, the above condition takes the form:

$$\vec{\Pi}(\widetilde{\mathbf{v}}_\beta) = -\vec{\Pi}(\langle \mathbf{v}_\beta \rangle^\beta) \quad \text{at } \mathbf{A}_{\beta\sigma}. \tag{49}$$

Therefore, Eqs. (47) and (49) provide

$$\widetilde{\mathbf{v}}_\beta = -\langle \mathbf{v}_\beta \rangle^\beta \quad \text{at } \mathbf{A}_{\beta\sigma}, \tag{50}$$

which corresponds to a no-slip and no-penetration condition ($\mathbf{v}_\beta = 0$) at the solid–liquid interface. As it will be seen in the following analysis, the boundary condition (50) will play a key role in the closed form of Eqs. (11), (43). Indeed, from (50) we deduce that the order of magnitude of the velocity deviation $\widetilde{\mathbf{v}}_\beta$ can be estimated by:

$$\widetilde{\mathbf{v}}_\beta = \mathrm{O}(\langle \mathbf{v}_\beta \rangle^\beta). \tag{51}$$

Under these circumstances, the continuity equation (44) can be simplified on the basis of the order of magnitude estimates of the different terms of this equation. The three terms in (44) involving $\widetilde{\mathbf{v}}_\beta$ or $\langle \mathbf{v}_\beta \rangle^\beta$ can easily be evaluated by:

$$\varepsilon_\beta \rho_\beta \nabla \cdot \widetilde{\mathbf{v}}_\beta = \mathrm{O}\left(\varepsilon_\beta \rho_\beta \frac{\langle \mathbf{v}_\beta \rangle^\beta}{\ell_\beta} \right), \tag{52}$$

$$\varepsilon_\beta \widetilde{\mathbf{v}}_\beta \cdot \nabla \rho_\beta = \mathrm{O}\left(\varepsilon_\beta \langle \mathbf{v}_\beta \rangle^\beta \frac{\rho_\beta}{L} \right), \tag{53}$$

$$\rho_\beta \nabla \varepsilon_\beta \cdot \langle \mathbf{v}_\beta \rangle^\beta = \mathrm{O}\left(\varepsilon_\beta \rho_\beta \frac{\langle \mathbf{v}_\beta \rangle^\beta}{L_\varepsilon} \right) \tag{54}$$

and according to the length scale constraint (8), we conclude:

$$\varepsilon_\beta \widetilde{\mathbf{v}}_\beta \cdot \nabla \rho_\beta, \rho_\beta \nabla \varepsilon_\beta \cdot \langle \mathbf{v}_\beta \rangle^\beta \ll \varepsilon_\beta \rho_\beta \nabla \cdot \widetilde{\mathbf{v}}_\beta. \tag{55}$$

Furthermore, if $\overline{w}_n$ represents the averaged interfacial growth velocity defined by:

$$\overline{w}_n = \frac{1}{A} \int_{A_{\beta\sigma}} \mathbf{n}_{\beta\sigma} \cdot \mathbf{w}_{\beta\sigma} \, \mathrm{d}A \tag{56}$$

the macroscopic mass balance (15), with $\mathbf{v}_\sigma = 0$, provides the following estimation of the melting rate $\dot{m}_\beta$:

$$\dot{m}_\beta = -\dot{m}_\sigma \sim \rho_\sigma A_v \overline{w}_n = \mathrm{O}\left(\varepsilon_\beta \rho_\sigma \frac{\overline{w}_n}{\ell_\beta} \right), \tag{57}$$

where $A_v = A_{\beta\sigma}/V$ is the specific area estimated by Carbonell and Whitaker [45]:

$$A_v = \mathrm{O}\left(\frac{\varepsilon_\beta}{\ell_\beta} \right). \tag{58}$$

Regarding the term involving the time derivative of ε_β in Eqs. (44), (14) gives rise to:

$$\frac{\partial \varepsilon_\beta}{\partial t} = \frac{1}{V} \int_{A_{\beta\sigma}} \mathbf{n}_{\beta\sigma} \cdot \mathbf{w}_{\beta\sigma} \, \mathrm{d}A = -A_v \overline{w}_n = \mathrm{O}\left(\varepsilon_\beta \frac{\overline{w}_n}{\ell_\beta} \right). \tag{59}$$

Let us recall that we have assumed that the growth velocity $\mathbf{n}_{\beta\sigma} \cdot \mathbf{w}_{\beta\sigma}$ is generally small compared to the average velocity $\langle \mathbf{v}_\beta \rangle^\beta$ induced by natural convection. Therefore we have

$$|\overline{w}_n| \ll \| \langle \mathbf{v}_\beta \rangle^\beta \| \tag{60}$$

and Eqs. (52), (57), (59) and (60) give rise to the comparison:

$$\rho_\beta \frac{\partial \varepsilon_\beta}{\partial t}, \quad \dot{m}_\beta \ll \varepsilon_\beta \rho_\beta \nabla \cdot \widetilde{\mathbf{v}}_\beta. \tag{61}$$

Finally, Eq. (44) reduces to the simple form:

$$\nabla \cdot \widetilde{\mathbf{v}}_\beta = 0. \tag{62}$$

3.2. Momentum equation

In order to derive the local momentum closure equation we introduce Gray's decomposition for the velocity and the pressure in (2) and we subtract the averaged momentum equation (43). After straightforward manipulations, the closure problem, including the simplified boundary condition (50), takes the form:

$$\begin{aligned}
&\varepsilon_\beta \rho_\beta \frac{\partial \widetilde{\mathbf{v}}_\beta}{\partial t} + \varepsilon_\beta \rho_\beta \mathbf{v}_\beta \cdot \nabla \widetilde{\mathbf{v}}_\beta + \varepsilon_\beta \rho_\beta \widetilde{\mathbf{v}}_\beta \cdot \nabla \langle \mathbf{v}_\beta \rangle^\beta \\
&\quad - \nabla \cdot (\varepsilon_\beta \rho_\beta \langle \widetilde{\mathbf{v}}_\beta \widetilde{\mathbf{v}}_\beta \rangle^\beta) - \dot{m}_\beta \langle \mathbf{v}_\beta \rangle^\beta \\
&\quad - \frac{1}{V} \int_{A_{\beta\sigma}} \mathbf{n}_{\beta\sigma} \cdot (\mathbf{v}_\beta - \mathbf{w}_{\beta\sigma}) \rho_\beta \mathbf{v}_\beta \, \mathrm{d}A \\
&\quad = -\varepsilon_\beta \nabla \widetilde{P}_\beta + \varepsilon_\beta \mu_\beta \nabla^2 \widetilde{\mathbf{v}}_\beta \\
&\qquad - \frac{1}{V} \int_{A_{\beta\sigma}} \mathbf{n}_{\beta\sigma} \cdot (-\widetilde{P}_\beta \mathbf{I} + \mu_\beta \nabla \widetilde{\mathbf{v}}_\beta) \, \mathrm{d}A \\
&\qquad - \mu_\beta \nabla \cdot \left[\frac{1}{V} \int_{A_{\beta\sigma}} \mathbf{n}_{\beta\sigma} \widetilde{\mathbf{v}}_\beta \, \mathrm{d}A \right],
\end{aligned} \tag{63}$$

$$\widetilde{\mathbf{v}}_\beta = -\langle \mathbf{v}_\beta \rangle^\beta \quad \text{at } \mathbf{A}_{\beta\sigma}. \tag{64}$$

Eq. (63) is extremely complex, but as previously done for the continuity equation, it can be simplified by estimating the order of magnitude of its different terms. On the basis of the constraints (8), (51) and (60) let us examine each term of Eq. (63).

According to Quintard and Whitaker [52], if $\widetilde{t}$ and t^* represent the characteristic time variations of $\widetilde{\mathbf{v}}_\beta$ and $\langle \mathbf{v}_\beta \rangle^\beta$, respectively, we can assume time scales separation:

$$\widetilde{t} \ll t^* \tag{65}$$

that leads to neglect $\partial \widetilde{\mathbf{v}}_\beta / \partial t$ when solving the coupled equations (43) and (63) . The convective and dispersive terms are easily estimated by:

$$\varepsilon_\beta \rho_\beta \mathbf{v}_\beta \cdot \nabla \widetilde{\mathbf{v}}_\beta = \mathrm{O}\left(\varepsilon_\beta \rho_\beta \frac{(\langle \mathbf{v}_\beta \rangle^\beta)^2}{\ell_\beta} \right), \tag{66}$$

$$\varepsilon_\beta \rho_\beta \widetilde{\mathbf{v}}_\beta \cdot \nabla \langle \mathbf{v}_\beta \rangle^\beta = \mathrm{O}\left(\varepsilon_\beta \rho_\beta \frac{(\langle \mathbf{v}_\beta \rangle^\beta)^2}{L_v} \right), \tag{67}$$

$$\nabla \cdot (\varepsilon_\beta \rho_\beta \langle \widetilde{\mathbf{v}}_\beta \widetilde{\mathbf{v}}_\beta \rangle^\beta = \mathrm{O}\left(\varepsilon_\beta \rho_\beta \frac{(\langle \mathbf{v}_\beta \rangle^\beta)^2}{L} \right), \tag{68}$$

where L associated to macroscopic spatial variations, is assumed to be such that $L \sim L_v$. Using the length-scale constraint given by Eq. (8) leads to

$$\nabla \cdot (\varepsilon_\beta \rho_\beta \langle \widetilde{\mathbf{v}}_\beta \widetilde{\mathbf{v}}_\beta \rangle^\beta \sim \varepsilon_\beta \rho_\beta \widetilde{\mathbf{v}}_\beta \cdot \nabla \langle \mathbf{v}_\beta \rangle^\beta \ll \varepsilon_\beta \rho_\beta \mathbf{v}_\beta \cdot \nabla \widetilde{\mathbf{v}}_\beta. \tag{69}$$

The two other terms in the left-hand side of Eq. (63) represent the momentum transfer due to phase change. Since the liquid velocity at the solid–liquid interface induced by volume change has been neglected (we recall that boundary condition (64) has been derived on the basis of this assumption), the interfacial momentum transfer (area integral) is therefore also negligible

$$\frac{1}{V} \int_{A_{\beta\sigma}} \rho_\beta \mathbf{n}_{\beta\sigma} \cdot (\mathbf{v}_\beta - \mathbf{w}_{\beta\sigma}) \mathbf{v}_\beta \, \mathrm{d}A \simeq 0. \tag{70}$$

Using the estimation of the solidification rate given by Eq. (57), the second phase change term $\dot{m}_\beta\langle\mathbf{v}_\beta\rangle^\beta$ in (63) is estimated by:

$$\dot{m}_\beta\langle\mathbf{v}_\beta\rangle^\beta = \mathrm{O}\left(\rho_\sigma\frac{\overline{w}_n\varepsilon_\beta\langle\mathbf{v}_\beta\rangle^\beta}{\ell_\beta}\right) \tag{71}$$

and according to (60) and (66), we have:

$$\dot{m}_\beta\langle\mathbf{v}_\beta\rangle^\beta \ll \varepsilon_\beta\rho_\beta\mathbf{v}_\beta\cdot\nabla\widetilde{\mathbf{v}}_\beta. \tag{72}$$

Finally, $\varepsilon_\beta\rho_\beta\mathbf{v}_\beta\cdot\nabla\widetilde{\mathbf{v}}_\beta$ is the only significant term remaining on the left-hand side of (63).

Regarding the right-hand side of Eq. (63), the first three terms have already been estimated by [38] and details can be found in this reference. All these terms have the same order of magnitude, for example the interfacial momentum exchange is such that:

$$\frac{1}{V}\int_{A_{\beta\sigma}}\mathbf{n}_{\beta\sigma}\cdot(-\widetilde{P}_\beta\mathbf{I}+\mu_\beta\nabla\widetilde{\mathbf{v}}_\beta)\,\mathrm{d}A = \mathrm{O}\left(\varepsilon_\beta\mu_\beta\frac{\langle\mathbf{v}_\beta\rangle^\beta}{\ell_\beta^2}\right), \tag{73}$$

where it is assumed that the contribution of the pressure $\widetilde{P}_\beta$ in the integral is not greater than the contribution of the velocity term and where Eq. (73) takes into account the boundary condition (51) at $\mathbf{A}_{\beta\sigma}$. This latter condition at the $\mathbf{A}_{\beta\sigma}$ interface allows to write the last term of Eq. (63) under the form

$$\mu_\beta\nabla\cdot\left[\frac{1}{V}\int_{A_{\beta\sigma}}\mathbf{n}_{\beta\sigma}\widetilde{\mathbf{v}}_\beta|_{\mathbf{r}}\,\mathrm{d}A\right] = \mu_\beta\nabla\cdot\left[\frac{1}{V}\int_{A_{\beta\sigma}}\mathbf{n}_{\beta\sigma}\langle\mathbf{v}_\beta\rangle^\beta|_{\mathbf{r}}\,\mathrm{d}A\right] \tag{74}$$

and using Eq. (40) leads to

$$\mu_\beta\nabla\cdot\left[\frac{1}{V}\int_{A_{\beta\sigma}}\mathbf{n}_{\beta\sigma}\widetilde{\mathbf{v}}_\beta|_{\mathbf{r}}\,\mathrm{d}A\right] = \mu_\beta\nabla\cdot[\nabla\varepsilon_\beta\langle\mathbf{v}_\beta\rangle^\beta]. \tag{75}$$

Finally, (75) can be estimated by:

$$\mu_\beta\nabla\cdot\left[\frac{1}{V}\int_{A_{\beta\sigma}}\mathbf{n}_{\beta\sigma}\widetilde{\mathbf{v}}_\beta|_{\mathbf{r}}\,\mathrm{d}A\right] = \mu_\beta\nabla\varepsilon_\beta\cdot\nabla\langle\mathbf{v}_\beta\rangle^\beta+\mu_\beta\nabla^2\varepsilon_\beta\langle\mathbf{v}_\beta\rangle^\beta \tag{76}$$

$$= \mathrm{O}\left(\varepsilon_\beta\mu_\beta\frac{\langle\mathbf{v}_\beta\rangle^\beta}{L_vL_\varepsilon}\right);\mathrm{O}\left(\varepsilon_\beta\mu_\beta\frac{\langle\mathbf{v}_\beta\rangle^\beta}{L_\varepsilon^2}\right), \tag{77}$$

where the porosity gradients are explicitly present. At this stage, it is important to recall that the length scale constraint used in the case of mushy zone with moderate evolving heterogeneities is defined by:

$$\ell_\beta \ll L_\varepsilon \tag{78}$$

and therefore, from (73), (77) and (78), we obtain

$$\varepsilon_\beta\mu_\beta\nabla^2\widetilde{\mathbf{v}}_\beta \sim -\frac{1}{V}\int_{A_{\beta\sigma}}\mathbf{n}_{\beta\sigma}\cdot(-\widetilde{P}_\beta\mathbf{I}+\mu_\beta\nabla\widetilde{\mathbf{v}}_\beta)\,\mathrm{d}A \gg \mu_\beta\nabla\cdot\left[\frac{1}{V}\int_{A_{\beta\sigma}}\mathbf{n}_{\beta\sigma}\widetilde{\mathbf{v}}_\beta\,\mathrm{d}A\right]. \tag{79}$$

Finally, the closure momentum equation (63) reduces to

$$\rho_\beta\mathbf{v}_\beta\cdot\nabla\widetilde{\mathbf{v}}_\beta = -\nabla\widetilde{P}_\beta+\mu_\beta\nabla^2\widetilde{\mathbf{v}}_\beta - \frac{1}{V}\int_{A_{\beta\sigma}}\mathbf{n}_{\beta\sigma}\cdot(-\widetilde{P}_\beta\mathbf{I}+\mu_\beta\nabla\widetilde{\mathbf{v}}_\beta)\,\mathrm{d}A. \tag{80}$$

3.3. Local closure problem

We summarize the closure problem constituted by the equations derived in the previous section associated to the interface condition at $\mathbf{A}_{\beta e}$:

$$\nabla\cdot\widetilde{\mathbf{v}}_\beta = 0, \tag{81}$$

$$\rho_\beta\mathbf{v}_\beta\cdot\nabla\widetilde{\mathbf{v}}_\beta = -\nabla\widetilde{P}_\beta+\mu_\beta\nabla^2\widetilde{\mathbf{v}}_\beta - \frac{1}{V}\int_{A_{\beta\sigma}}\mathbf{n}_{\beta\sigma}\cdot(-\widetilde{P}_\beta\mathbf{I}+\mu_\beta\nabla\widetilde{\mathbf{v}}_\beta)\,\mathrm{d}A, \tag{82}$$

$$\widetilde{\mathbf{v}}_\beta = -\underbrace{\langle\mathbf{v}_\beta\rangle^\beta}_{\text{source}} \quad \text{at } \mathbf{A}_{\beta\sigma}, \tag{83}$$

$$\widetilde{\mathbf{v}}_\beta = g(\mathbf{r},t) \quad \text{at } \mathbf{A}_{\beta e}. \tag{84}$$

In the above problem, the boundary condition given by Eq. (84) is not known a priori but according to Eq. (51) we know that $g(\mathbf{r},t)$ is of the order of $\langle\mathbf{v}_\beta\rangle^\beta$ and we do know that this condition will influence the $\widetilde{\mathbf{v}}_\beta$-field only in a region of thickness ℓ_β at the boundary of the averaging volume V [53]. That is the reason why, for homogeneous porous structures, the closure problem is generally solved in a representative region (unit cell) with periodicity conditions at the boundary $\mathbf{A}_{\beta e}$

$$\widetilde{P}_\beta(\mathbf{r}+\ell_i) = \widetilde{P}_\beta(\mathbf{r}), \quad \widetilde{\mathbf{v}}_\beta(\mathbf{r}+\ell_i) = \widetilde{\mathbf{v}}_\beta(\mathbf{r}) \quad \text{with } i = 1,2,3 \tag{85}$$

assuming that variations of $\langle\mathbf{v}_\beta\rangle^\beta$ can be neglected within the unit cell. In Eq. (85), ℓ_i represents the lattice vectors. In the case of columnar dendritic porous structures, macroscopic properties (porosity, permeability, etc.) are continuously space-dependent (evolving heterogeneities) and the periodicity condition in the direction parallel to the primary dendrite arms seems to be inappropriate. Actually, the type of boundary condition at $\mathbf{A}_{\beta e}$ depends on the geometry of the dendritic structure and therefore on its decreasing rate τ. Indeed, [32,37] have shown that for small or moderate values of this parameter, the periodicity condition could be a relevant approximation, especially if we do remember that due to the small scale of influence of (84), such a condition is mathematically

weak in our problem. Finally, the local closure problem for a columnar dendritic mushy zone presenting small or moderate evolving heterogeneities is given by Eqs. (81)–(83) and (85). Under this form, this problem takes the same form as the closure problem given by [53] in the absence of phase change. This important conclusion means that the contribution of "moderate" (but not negligible) evolving heterogeneities and solid–liquid phase change in solidifying mushy zone hardly influence the determination of the effective transport properties of this region. However, we will see in Section 4, that these contributions at the macroscopic scale are not necessarily negligible. For the sake of clarity, the main steps of the treatment of the system (81)–(85) are briefly recalled in Appendix B and all the details can be found in [53].

4. Closed form of the momentum equation

Using the macroscopic mass conservation equation (11) within Eq. (43) according to simplifications (70) and Eqs. (76), (B.1) and (B.5), we obtain the non-conservative closed form of the averaged momentum equation:

$$\begin{aligned}
&\varepsilon_\beta\rho_\beta\frac{\partial\langle\mathbf{v}_\beta\rangle^\beta}{\partial t}+\varepsilon_\beta\rho_\beta\langle\mathbf{v}_\beta\rangle^\beta\cdot\nabla\langle\mathbf{v}_\beta\rangle^\beta\\
&\quad+\nabla\cdot\left[\varepsilon_\beta\rho_\beta\langle\mathbf{v}_\beta\rangle^\beta\cdot\langle\mathbf{M}^t\mathbf{M}\rangle^\beta\cdot\langle\mathbf{v}_\beta\rangle^\beta\right]+\dot{m}_\beta\langle\mathbf{v}_\beta\rangle^\beta\\
&=-\varepsilon_\beta\langle P_\beta\rangle^\beta+\varepsilon_\beta\mu_\beta\nabla^2\langle\mathbf{v}_\beta\rangle^\beta+\mu_\beta\nabla\varepsilon_\beta\cdot\nabla\langle\mathbf{v}_\beta\rangle^\beta\\
&\quad+\mu_\beta\nabla^2\varepsilon_\beta\langle\mathbf{v}_\beta\rangle^\beta-\varepsilon_\beta^2\mu_\beta\mathbf{K}^{-1}.\langle\mathbf{v}_\beta\rangle^\beta-\varepsilon_\beta^2\mu_\beta\mathbf{K}^{-1}.\mathbf{F}.\langle\mathbf{v}_\beta\rangle^\beta\\
&\quad+\varepsilon_\beta\rho_\beta\mathbf{g}
\end{aligned}\tag{86}$$

Some terms of Eq. (86) need to be discussed in the context of columnar dendritic-like porous structure since their influence depends on the position within the mushy zone.

4.1. Inertia terms

It is well known that flows in porous media for small pore-scale Reynolds numbers are governed by Darcy's law which supposes a linear relationship between the average pressure gradient and the seepage velocity $\langle\mathbf{v}_\beta\rangle$ [54,55]. The transition between Darcy's regime where viscous forces prevail and the inertial regime takes place for seepage Reynolds numbers between 1 and 10, and the inertial effects are traditionaly represented by Forchheimer's correction [56]. The problem of the correct quadratic or cubic form of this term at small Reynolds numbers is not discussed here [57,58]. The macroscopic momentum Eq. (86) derived in this study involves three inertia terms which need to be compared:

$$\begin{aligned}
&\varepsilon_\beta\rho_\beta\langle\mathbf{v}_\beta\rangle^\beta\cdot\nabla\langle\mathbf{v}_\beta\rangle^\beta\\
&\quad\text{macroscopic convective flux,}\\
&\nabla\cdot[\varepsilon_\beta\rho_\beta\langle\mathbf{v}_\beta\rangle^\beta\cdot\langle\mathbf{M}^t\mathbf{M}\rangle^\beta\cdot\langle\mathbf{v}_\beta\rangle^\beta]\\
&\quad\text{momentum dispersive flux,}\\
&-\varepsilon_\beta^2\mu_\beta\mathbf{K}^{-1}\cdot\mathbf{F}\cdot\langle\mathbf{v}_\beta\rangle^\beta\\
&\quad\text{Forchheimer or microscopic inertial effects.}
\end{aligned}\tag{87}$$

Since the columnar dendritic mushy zone is characterized by continuous spatial variations of the macroscopic properties (liquid volume fraction and permeability), and if the Reynolds number is greater than 1, two regions have to be considered.

First, for small or intermediate porosity values, the estimation:

$$\widetilde{\mathbf{v}}_\beta=\mathrm{O}(\langle\mathbf{v}_\beta\rangle^\beta)\tag{88}$$

provides

$$\mathbf{M}=\mathrm{O}(1)\tag{89}$$

and therefore

$$\begin{aligned}
&\nabla\cdot\left[\varepsilon_\beta\rho_\beta\langle\mathbf{v}_\beta\rangle^\beta\cdot\langle\mathbf{M}^t\mathbf{M}\rangle^\beta\cdot\langle\mathbf{v}_\beta\rangle^\beta\right]\\
&\quad\sim\varepsilon_\beta\rho_\beta\langle\mathbf{v}_\beta\rangle^\beta\cdot\nabla\langle\mathbf{v}_\beta\rangle^\beta=\mathrm{O}\left(\varepsilon_\beta\rho_\beta\frac{(\langle\mathbf{v}_\beta\rangle^\beta)^2}{L}\right),
\end{aligned}\tag{90}$$

while the estimation of the Forchheimer correction leads to [53]

$$\mu_\beta\varepsilon_\beta^2\mathbf{K}^{-1}\cdot\mathbf{F}\cdot\langle\mathbf{v}_\beta\rangle^\beta=\mathrm{O}\left(\frac{(\langle\mathbf{v}_\beta\rangle^\beta)^2}{\ell_\beta}\right).\tag{91}$$

Hence, due to the length scale constraint (8) it is clear that the most important term describing inertial effects is given by the Forchheimer correction. This phenomenon is attributed to the microscopic drag forces which are much more important than the macroscopic inertial effects [59,60].

The second case concerns the region near the tip of the dendrites where the porosity tends towards unity and the notion of dispersion does not make sense any more. Since the permeability becomes infinite, the Forchheimer correction does not play any role, and the only remaining inertia term is the usual convective term: this corresponds to the situation described by the classical Navier–Stokes equation. Therefore, whatever the porosity in the columnar dendritic mushy zone, the dispersive flux given by the quantity $\nabla\cdot[\varepsilon_\beta\rho_\beta\langle\mathbf{v}_\beta\rangle^\beta\cdot\langle\mathbf{M}^t\mathbf{M}\rangle^\beta\cdot\langle\mathbf{v}_\beta\rangle^\beta]$ is negligible and inertia phenomena is described by the Forchheimer correction for *small and moderate* porosity while they will be represented by the macroscopic convective term $\rho_\beta\langle\mathbf{v}_\beta\rangle^\beta\cdot\nabla\langle\mathbf{v}_\beta\rangle^\beta$ in the vicinity of dendrite tips.

Finally, since the interfacial momentum transfer due to phase change (70) can be discarded, the final form of the macroscopic mass and momentum conservation equations written in term of superficial velocity (filtration velocity) take the final form:

$$\frac{\partial}{\partial t}(\varepsilon_\beta \rho_\beta + \varepsilon_\sigma \rho_\sigma) + \nabla \cdot (\rho_\beta \langle \mathbf{v}_\beta \rangle) = 0, \tag{92}$$

$$\begin{aligned}
&\varepsilon_\beta^{-1} \frac{\partial}{\partial t}(\rho_\beta \langle \mathbf{v}_\beta \rangle) + \varepsilon_\beta^{-1} \nabla \cdot \left(\varepsilon_\beta^{-1} \rho_\beta \langle \mathbf{v}_\beta \rangle \langle \mathbf{v}_\beta \rangle \right) \\
&\quad = -\langle P_\beta \rangle^\beta + \rho_\beta \mathbf{g} + \mu_\beta \varepsilon_\beta^{-1} \nabla^2 \langle \mathbf{v}_\beta \rangle \\
&\qquad - \underbrace{\mu_\beta \varepsilon_\beta^{-1} \nabla \varepsilon_\beta . \nabla (\varepsilon_\beta^{-1} \langle \mathbf{v}_\beta \rangle)}_{\text{Second Brinkman correction term}} - \mu_\beta \mathbf{K}^{-1} \cdot \langle \mathbf{v}_\beta \rangle \\
&\qquad - \mu_\beta \mathbf{K}^{-1} \cdot \mathbf{F} \cdot \langle \mathbf{v}_\beta \rangle.
\end{aligned} \tag{93}$$

4.2. Brinkman correction terms

Under this form, Eq. (93) includes the second Brinkman correction term that explicitly involves porosity gradients. Using intrinsic velocity, similar terms (actually, three Brinkman correction terms instead of two) have been derived by Whitaker [38] and Quintard and Whitaker [46] in the absence of phase-change and for homogeneous structures. They are generally neglected due to the length-scale constraint (5) in such a geometry.

In the case of columnar dendritic-like porous structures the spatial porosity variations are generally progressive and two situations have to be considered. First, for small decreasing rates of the geometry (quasi-homogeneous porous structures) where scale separation is given by Eq. (6), the two Brinkman terms in Eq. (93) do not contribute to momentum transport except near the tip of the dendrites where the liquid volume fraction is close to one and where the first Brinkman term is essential to account for viscous diffusion phenomena. In the case of a dendritic mushy zone presenting larger (but moderate) evolving heterogeneities, scale separation is represented by the length-scale constraint (7). In this situation, we have shown (assuming $L_\varepsilon \sim L_v$) that the order of magnitude of the Brinkman terms is not small compared to the other terms and could have a non-negligible influence on the momentum, heat and mass transport within the mushy zone. Numerical simulation taking into account the porosity gradient are under development in order to quantify their actual influence. Finally, for rapid spatial changes of the porosity at the mush–fluid region interface, the second Brinkman correction could be replaced by a jump condition [61].

Obviously, retaining the porosity gradients in the macroscopic momentum equation would provide a much more complex closure problem where these terms would be present as source terms for the deviation fields. In this case, the closure problem becomes a *non-local* problem and its resolution still remains a challenge. However, for *moderate decreasing rates* of the geometry, τ, Goyeau et al. [32] have shown that even if the porosity gradients are present at the macroscopic scale, their contribution at the local scale can be neglected in the closure problem leading to an acceptable approximation of the spatial variation of the permeability.

All this analysis has been performed for laminar flow regimes and needs to be extended to turbulent flows where fluctuations $\tilde{\mathbf{v}}_\beta$ involving dispersion phenomena can be much more important and therefore non negligible [62].

5. Conclusion

A new derivation of the macroscopic momentum equation for an interdendritic flow through a solidifying columnar mushy zone has been carried out using an averaging procedure with *local closure problem*. In order to simplify such a complex problem, all the terms arising from the averaging process (micro- and macro-contributions to momentum transport) have been estimated and compared on the basis of the characteristic length scale constraints associated with dendritic-like porous structures presenting evolving heterogeneities. For dendritic structures with "moderate" (but not small) decreasing rate of the geometry, we have shown that heterogeneities and phase change hardly influence the description of effective properties (permeability and inertia tensor) of the dendritic layer. Whatever the porosity within the columnar mushy zone, the macroscopic dispersive flux has been found to be negligible compared to other inertial terms of the closed form of the momentum conservation equation. Therefore, inertial phenomena will be described by the Forchheimer correction for small and moderate porosity while they will be represented by the macroscopic convective term near the top of the dendrites where porosity is close to one. Finally, the closed form of the macroscopic momentum transport equation includes a second Brinkman correction term explicitly involving porosity gradients. In some cases depending on the decreasing rate of the geometry, this additional term could significantly modify the representation of the momentum, heat and mass transfer in the mushy zone.

This work is a first step towards the derivation of a "complete" macroscopic model for the simulation of multi-component solidification systems and a similar work concerning the heat and species transfer conservation equations and the determination of effective transport properties in the mushy zone (diffusion–dispersion, mass exchange and conductivity coefficients) is presently under development. One of the application we are involved in, concerns the solidification of a molten pool (corium) that can be found in a nuclear reactor

vessel during a scenario of an hypothetical severe accident [63].

Acknowledgements

This work is supported by IPSN (Department DRS/SEMAR) under research contract number: 402048-B002850. B.G. thanks Professor Stephen Whitaker (Department of Chemical Engineering, University of California at Davis, USA) for fruitful discussions and comments. Two of the authors (P.B-M. and F.F.) wish to gratefully acknowledge Bruno Piar for his availability and his contribution to the discussion.

Appendix A. The volume-averaging technique

Here, we briefly recall the main features of the volume averaging theory and all the details are provided in [22,23,44,45,64], and many subsequent papers.

Let us consider a physical property ψ, continuous in each phase of a β–σ system:

$$\psi = \begin{cases} \psi_\beta & \text{in } \beta\text{-phase}, \\ \psi_\sigma & \text{in } \sigma\text{-phase}. \end{cases} \tag{A.1}$$

In (A.1), ψ_β and ψ_σ are defined such as:

$$\begin{aligned} &\psi_\beta = 0 \quad \text{in } \sigma\text{-phase}, \\ &\psi_\sigma = 0 \quad \text{in } \beta\text{-phase}. \end{aligned} \tag{A.2}$$

The technique consists in averaging ψ in a representative elementary volume (REV) or averaging volume V of a two-phase system (Fig. 1). The following definitions are used:

$$\begin{aligned} &V: \text{ averaging volume}, \\ &V_\beta: \text{ volume of } \beta\text{-phase within } V, \\ &V_\sigma: \text{ volume of } \sigma\text{-phase within } V. \end{aligned} \tag{A.3}$$

The phase volume fractions are defined as:

$$\varepsilon_\beta = \frac{V_\beta}{V}, \quad \varepsilon_\sigma = \frac{V_\sigma}{V} \tag{A.4}$$

and related by

$$\varepsilon_\beta + \varepsilon_\sigma = 1. \tag{A.5}$$

A better definition of these quantities involves the phase indicator defined as

$$\gamma_\beta = \begin{cases} 1 & \text{in } \beta\text{-phase}, \\ 0 & \text{in } \sigma\text{-phase} \end{cases} \tag{A.6}$$

in the case of the β-phase. Using this definition, the β-phase volume fraction is simply

$$\varepsilon_\beta = \langle \gamma_\beta \rangle. \tag{A.7}$$

The superficial volume average of ψ_β is defined as:

$$\langle \psi_\beta \rangle|_{\mathbf{x}} = \frac{1}{V} \int_{V_\beta} \psi_\beta(\mathbf{x} + \mathbf{y}_\beta)\, \mathrm{d}V_y. \tag{A.8}$$

The intrinsic phase average of ψ_β is defined as:

$$\langle \psi_\beta \rangle^\beta|_{\mathbf{x}} = \frac{1}{V_\beta} \int_{V_\beta} \psi_\beta(\mathbf{x} + \mathbf{y}_\beta)\, \mathrm{d}V_y. \tag{A.9}$$

The notation dV_y is used to indicate that the integration is done with respect to the variable $\mathbf{y}$ (Fig. 1). Note that both types of averages are calculated at the centroid $\mathbf{x}$ of the averaging volume. However, for convenience, the point $\mathbf{x}$ is usually not specified, and the following notations are adopted:

$$\langle \psi_\beta \rangle = \langle \psi_\beta \rangle|_{\mathbf{x}}, \tag{A.10}$$

$$\langle \psi_\beta \rangle^\beta = \langle \psi_\beta \rangle^\beta|_{\mathbf{x}}. \tag{A.11}$$

These two kinds of averages are related by:

$$\langle \psi_\beta \rangle = \varepsilon_\beta \langle \psi_\beta \rangle^\beta. \tag{A.12}$$

According to [44], ψ_β can be decomposed in two parts:

$$\psi_\beta = \gamma_\beta \langle \psi_\beta \rangle^\beta + \widetilde{\psi}_\beta, \tag{A.13}$$

where $\langle \psi_\beta \rangle^\beta$ and $\widetilde{\psi}_\beta$ are the averaged and the deviation (fluctuation), respectively.

In order to average the microscopic conservation equations in each phase, one uses the following theorems [44] which relate the superficial volume average of the spatial and temporal partial derivatives to the partial derivatives of the superficial volume average:

$$\langle \nabla \psi_\beta \rangle = \nabla \langle \psi_\beta \rangle + \frac{1}{V} \int_{A_{\beta\sigma}} \mathbf{n}_{\beta\sigma} \psi_\beta \, \mathrm{d}A, \tag{A.14}$$

$$\left\langle \frac{\partial \psi_\beta}{\partial t} \right\rangle = \frac{\partial \langle \psi_\beta \rangle}{\partial t} - \frac{1}{V} \int_{A_{\beta\sigma}} \mathbf{n}_{\beta\sigma} \cdot \mathbf{w}_{\beta\sigma} \psi_\beta \, \mathrm{d}A, \tag{A.15}$$

where $\mathbf{w}_{\beta\sigma}$ is the local interface velocity and $\mathbf{n}_{\beta\sigma}$ is the unit normal vector at the β–σ interface, pointed from the β-phase towards the σ-phase (Fig. 1). For the demonstration of these theorems, one can refer to [65,22].

Appendix B. Closure problem

Due to the boundary condition (83) where $\langle \mathbf{v}_\beta \rangle^\beta$ can be considered as a source term in the boundary value problem for $\widetilde{P}_\beta$ and $\widetilde{\mathbf{v}}_\beta$, the following solutions are proposed for the deviation fields:

$$\widetilde{\mathbf{v}}_\beta = \mathbf{M} \cdot \langle \mathbf{v}_\beta \rangle^\beta, \tag{B.1}$$

$$\widetilde{P}_\beta = \mu_\beta \mathbf{m} \cdot \langle \mathbf{v}_\beta \rangle^\beta, \tag{B.2}$$

where **m** and **M** are vector and tensor fields, respectively. In order to separate linear and inertia effects [53] decomposed **m** and **M** in two parts:

$$\mathbf{m} = \mathbf{b} + \mathbf{c}, \tag{B.3}$$

$$\mathbf{M} = \mathbf{B} + \mathbf{C} \tag{B.4}$$

and the closed form of the interfacial momentum exchange can be written under the generic form

$$\frac{1}{V}\int_{A_{\beta\sigma}} \mathbf{n}_{\beta\sigma}\cdot(-\widetilde{P}_\beta \mathbf{I} + \mu_\beta \nabla \widetilde{\mathbf{v}}_\beta)\,\mathrm{d}A = \underbrace{-\varepsilon_\beta^2 \mu_\beta \mathbf{K}^{-1}\cdot\langle \mathbf{v}_\beta\rangle^\beta}_{\text{Darcy term}} \underbrace{-\varepsilon_\beta^2 \mu_\beta \mathbf{K}^{-1}\cdot\mathbf{F}\cdot\langle \mathbf{v}_\beta\rangle^\beta}_{\text{Inertia term}}, \tag{B.5}$$

where **K** is the permeability tensor that only depends on the tortuosity of the porous structure and where **F** is the Forchheimer correction tensor which accounts for microscopic inertia effects [53]. These tensors can explicitly be written under the form:

$$\varepsilon_\beta \mathbf{K}^{-1} = -\frac{1}{V_\beta}\int_{A_{\beta\sigma}} \mathbf{n}_{\beta\sigma}\cdot(-\mathbf{I}\mathbf{b} + \nabla \mathbf{B})\,\mathrm{d}A, \tag{B.6}$$

$$\varepsilon_\beta^2 \mathbf{K}^{-1}\cdot\mathbf{F} = -\frac{1}{V_\beta}\int_{A_{\beta\sigma}} \mathbf{n}_{\beta\sigma}\cdot(-\mathbf{I}\mathbf{c} + \nabla \mathbf{C})\,\mathrm{d}A, \tag{B.7}$$

where the vector **b** and the tensor **B** are specified by the two periodic boundary problems [53]:

Problem I:

$$\nabla\cdot\mathbf{B} = 0, \tag{B.8}$$

$$0 = -\nabla\mathbf{b} + \nabla^2\mathbf{B} - \frac{1}{V_\beta}\int_{A_{\beta\sigma}} \mathbf{n}_{\beta\sigma}\cdot(-\mathbf{I}\mathbf{b} + \nabla\mathbf{B})\,\mathrm{d}A, \tag{B.9}$$

$$\mathbf{B} = -\mathbf{I} \quad \text{at } \mathbf{A}_{\beta\sigma}, \tag{B.10}$$

$$\mathbf{b}(\mathbf{r} + \ell_i) = \mathbf{b}(\mathbf{r}), \quad \mathbf{B}(\mathbf{r} + \ell_i) = \mathbf{B}(\mathbf{r}) \quad \text{at } \mathbf{A}_{\beta e}, \tag{B.11}$$

$$\langle \mathbf{B}\rangle^\beta = 0. \tag{B.12}$$

After straightforward manipulations, the system (B.8)–(B.12) can be written under the more convenient form [39]:

$$\nabla\cdot\mathbf{D} = 0, \tag{B.13}$$

$$-\nabla\mathbf{d} + \nabla^2\mathbf{D} = \mathbf{I}, \tag{B.14}$$

$$\mathbf{D} = 0 \quad \text{at } \mathbf{A}_{\beta\sigma}, \tag{B.15}$$

$$\mathbf{d}(\mathbf{r} + \ell_i) = \mathbf{d}(\mathbf{r}), \quad \mathbf{D}(\mathbf{r} + \ell_i) = \mathbf{D}(\mathbf{r}) \quad \text{at } \mathbf{A}_{\beta e} \tag{B.16}$$

$$\langle \mathbf{d}\rangle^\beta = 0, \quad \langle \mathbf{D}\rangle^\beta = -\varepsilon_\beta^{-1}\mathbf{K}, \tag{B.17}$$

where **D** and **d** are defined by:

$$\mathbf{D} = -\varepsilon_\beta^{-1}(\mathbf{B} + \mathbf{I})\cdot\mathbf{K}, \tag{B.18}$$

$$\mathbf{d} = -\varepsilon_\beta^{-1}\mathbf{b}\cdot\mathbf{K}. \tag{B.19}$$

The solution of the above problem does not raise major difficulties since the system given by Eqs. (B.13),(B.17)–(B.19) is similar to the classical Stokes boundary value problem where **d** and **D** would represent the pressure and the velocity, respectively. The resolution provides the **D**-field which is integrated to provide the permeability using the average condition (B.17).

The Forchheimer correction tensor **F** is calculated by solving Problem II, which depends both on the geometry of the porous structure but also on the intensity of the flow through the porous medium.

Problem II:

$$\nabla\cdot\mathbf{C} = 0, \tag{B.20}$$

$$\frac{\rho_\beta}{\mu_\beta}\mathbf{v}_\beta\cdot\nabla(\mathbf{B} + \mathbf{C}) = -\nabla\mathbf{c} + \nabla^2\mathbf{C} - \frac{1}{V_\beta}\int_{A_{\beta\sigma}} \mathbf{n}_{\beta\sigma}\cdot(-\mathbf{I}\mathbf{c} + \nabla\mathbf{C})\,\mathrm{d}A, \tag{B.21}$$

$$\mathbf{C} = 0 \quad \text{at } \mathbf{A}_{\beta\sigma}, \tag{B.22}$$

$$\mathbf{c}(\mathbf{r} + \ell_i) = \mathbf{c}(\mathbf{r}), \quad \mathbf{C}(\mathbf{r} + \ell_i) = \mathbf{C}(\mathbf{r}) \quad \text{at } \mathbf{A}_{\beta e}, \tag{B.23}$$

$$\langle \mathbf{C}\rangle^\beta = 0. \tag{B.24}$$

At this stage, a full solution of this problem is necessary to discuss seriously the dependence of **F** on the Reynolds number and the geometry. For instance, depending on the cases, a quadratic or a cubic dependence of the inertial correction to Darcy's law at *small Reynolds numbers* has been found [53,57,58,66]. According to Whitaker [53], the proposed boundary value problem is equivalent to the Navier–Stokes equations for steady, incompressible flow in a spatially periodic system. Numerical calculations are presently under development in order to study the relevance of the periodic boundary conditions at $\mathbf{A}_{\beta e}$ in the case of dendritic structures and to describe accurately the dependence of the Forchheimer correction.

References

[1] M. Flemings, Solidification Processing, McGraw-Hill, New York, 1974.

[2] M. Rappaz, V. Voller, Modeling of micro-macrosegregation in solidification processes, Met. Trans. A 21 (1990) 749–755.

[3] P. Prescott, F. Incropera, Convection heat and mass transfer in alloy solidification, Adv. Heat Transfer 28 (1996) 231–337.

[4] J. Szekely, A. Jassal, An experimental and analytical study of the solidification of a binry dendritic system, Met. Trans. B 9 (1978) 389–398.

[5] S. Ridder, S. Kou, R. Mehrabian, Effect of fluid flow on macrosegregation in axi-symmetric ingots, Met. Trans. B 12 (1981) 435–447.

[6] M. Worster, Natural convection in a mushy layer, J. Fluid Mech. 224 (1991) 335–359.
[7] M. Kaviany, Principles of Heat Transfer in Porous Media, Springer, Berlin, 1995.
[8] R. Hills, D. Loper, P. Roberts, A thermodynamically consistent model of a mushy zone, Quart. J. Mech. Appl. Math. 36 (1983) 505–539.
[9] W. Bennon, F. Incropera, A continuum model for momentum heat and species transport in binary solid–liquid phase change systems – I. Model formulation, Int. J. Heat Mass Transfer 30 (10) (1987) 2161–2170.
[10] P. Prescott, F. Incropera, W. Bennon, Modeling of dendritic solidification systems reassessment of the continuum momentum equation, Int. J. Heat Mass Transfer 34 (9) (1991) 2351–2359.
[11] S. Ganesan, D. Poirier, Conservation of mass and momentum for the flow of interdendritic liquid during solidification, Met. Trans. B 21 (1990) 173–181.
[12] J. Ni, C. Beckermann, A volume-averaged two-phase model for transport phenomena during solidification, Met. Trans. B 22 (1991) 349–361.
[13] T. Benihaddadene, Modélisation Macroscopique des écoulements et des Transferts dans un milieu poreux hétérogene: application à la solidification, Ph.D. Thesis, Université de Paris VI Mai, 1997.
[14] V. Voller, A. Brent, C. Prakash, The modelling of heat mass and solute transport in solidification systems, Int. J. Heat Mass Transfer 32 (9) (1989) 1719–1731.
[15] I. Kececioglu, B. Rubinsky, A continuum model for the propagation of discrete phase-change fronts in porous media in the presence of coupled heat flow fluid flow and species transport processes, Int. J. Heat Mass Transfer 32 (6) (1989) 1111–1130.
[16] P. Prescott, F. Incropera, D. Gaskell, The effects of undercooling, recalescence and solid transport on the solidification of binary metal alloys, Transport Phenom. Mater. Process. Manufact. 196 (1992) 31–39.
[17] W. Bennon, F. Incropera, A continuum model for momentum heat and species transport in binary solid–liquid phase change systems – II. Application to solidification in a rectangular cavity, Int. J. Heat Mass Transfer 30 (10) (1987) 2171–2187.
[18] W. Bennon, F. Incropera, The evolution of macrosegregation in statically cast binary ingots, Met. Trans. B 18 (1987) 611–616.
[19] M. Christenson, W. Bennon, F. Incropera, Solidification of an aqueous ammonium chloride solution in a rectangular cavity – II. Comparison of predicted and measured results, Int. J. Heat Mass Transfer 32 (1) (1989) 69–79.
[20] D.G Neilson, F.P. Incropera, Unidirectional solidification of a binary alloy and the effects of induced fluid motion, Int. J. Heat Mass Transfer 34 (7) (1991) 1717–1732.
[21] P. Prescott, F. Incropera, Convective transport phenomena and macrosegregation during solidification of a binary metal alloy: I–Numerical predictions, J. Heat Transfer 116 (1994) 735–741.
[22] S. Whitaker, Advances in theory of fluid motion in porous media, Ind. Eng. Chem. 61 (12) (1969) 14–28.
[23] J. Bear, Dynamics of Fluids in Porous Media, Dover, New York, 1972.
[24] C. Beckermann, R. Viskanta, Double-diffusive convection during dendritic solidification of a binary mixture, Physicochem. Hydrodyn. 10 (1988) 195–213.
[25] C. Beckermann, R. Viskanta, Mathematical modeling of transport phenomena during alloy solidification, Appl. Mech. Rev. 46 (1) (1993) 1–27.
[26] M. Schneider, C. Beckermann, A numerical study of the combined effects of microsegregation mushy zone permeability and flow, caused by volume contraction and thermosolutal convection, on macrosegregation and eutectic formation in binary alloy solidification, Int. J. Heat Mass Transfer 38 (18) (1995) 3455–3473.
[27] C. Beckermann, C. Wang, Mutiphase/scale modeling of alloy solidification, Annu. Rev. Heat Transfer 6 (1995) 115–198.
[28] A. Bensoussan, J.L. Lions, G. Papanicolaou, Asymptotic Analysis for Periodic Structures, North-Holland, Amsterdam, 1978.
[29] E. Sanchez, in: Non-homogeneous media and vibration theory, Lecture Notes in Physics, vol. 127, Springer, New York, 1980.
[30] W. Bennon, F. Incropera, An experimental investigation of binary solidification in a vertical channel with thermal and solutal mixed convection, J. Heat Transfer 111 (1989) 706–712.
[31] P. Prescott, F. Incropera, D. Gaskell, Convective transport phenomena and macrosegregation of a binary metal alloy: II – Experiments and comparisons with numerical predictions, J. Heat Transfer 116 (1994) 742–749.
[32] B. Goyeau, T. Benihaddadene, D. Gobin, M. Quintard, Averaged momentum equation for flow through a nonhomogeneous porous structure, Transport Porous Media 28 (1997) 19–50.
[33] P. Nandapurkar, D. Poirier, J. Heinrich, Momentum equation for dendritic solidification, Numer. Heat Transfer 19 (1991) 297–311.
[34] D. Poirier, Permeability for flow of interdendritic liquid in columnar–dendritic alloys, Met. Trans. B 18 (1987) 245–255.
[35] S. Ganesan, C. Chan, D. Poirier, Permeability for flow parallel to primary dendrite arms, Mater. Sci. Eng. A 151 (1992) 97–105.
[36] M. Bhat, D. Poirier, J. Heinrich, Permeability for cross flow through columnar–dendritic alloys, Met. Mater. Trans. B 26 (1995) 1049–1056.
[37] B. Goyeau, T. Benihaddadene, D. Gobin, M. Quintard, Numerical calculation of the permeability tensor in a dendritic mushy zone, Met. Mater. Trans. B 30 (1999) 613–622.
[38] S. Whitaker, Flow in porous media I: A theoretical derivation of Darcy's law, Transport Porous Media 1 (1986) 3–25.
[39] J. Barrère, O. Gipouloux, S. Whitaker, On the closure problem for Darcy's law, Transport Porous Media 7 (1992) 209–222.
[40] M. Quintard, S. Whitaker, Transport in ordered and disordered porous media III: Closure and comparison between theory and experiment, Transport Porous Media 15 (1994) 31–49.
[41] J. Cushman, On unifying the concept of scale, instrumentation, and stochastics in the development of multiphase

transport theory, Water Resour. Res. 20 (11) (1984) 1668–1676.
[42] H. Huppert, The fluid mechanics of solidification, J. Fluid Mech. 212 (1990) 209–240.
[43] R. Trivedi, K. Somboonsuk, Constrained dendritic growth and spacing, Mater. Sci. Eng. 65 (1984) 65–74.
[44] W. Gray, A derivation of the equations for multi-phase transport, Chem. Eng. Sci. 30 (1975) 229–233.
[45] R. Carbonell, S. Whitaker, in: Fundamentals of Transport Phenomena in Porous Media, Heat and Mass Transfer in Porous Media, Martinus Nijhoff, Dordrecht, 1984, pp. 121–198.
[46] M. Quintard, S. Whitaker, Transport in ordered and disordered porous media II: Generalized volume averaging, Transport Porous Media 14 (1994) 179–206.
[47] C. Misbah, Instabilité morphologique et convection solutale en solidification directionnelle des mélanges binaires dilués, Ph.D. Thesis, Université Paris VII mars, 1985.
[48] M. Krane, F. Incropera, Analysis of the effect of shrinkage on macrosegregation in alloy solidification, Met. Mater. Trans. A 26 (1995) 2329–2339.
[49] D. Poirier, K. Yeum, A. Maples, A thermodynamic prediction for microporosity formation in aluminium-rich Al–Cu alloys, Met. Trans. A 18 (1987) 1979–1987.
[50] D. Xu, Q. Li, Gravity- and solidification-shrinkage-induced liquid flow in a horizontally solidified alloy ingot, Numer. Heat Transfer A 20 (1991) 203–221.
[51] A. Chiareli, M. Worster, Flow focusing instability in a solidifying mushy layer, J. Fluid Mech. 297 (1995) 293–305.
[52] M. Quintard, S. Whitaker, Convection dispersion and interfacial transport of contaminants: homogeneous porous media, Adv. Water Resour. 17 (1994) 221–239.
[53] S. Whitaker, The Forchheimer equation: a theoretical development, Transport Porous Media 25 (1996) 27–61.
[54] V.D Cvetković, A continuum approach to high velocity flow in a porous medium, Transport Porous Media 1 (1986) 63–97.
[55] D. Nield, A. Bejan, Convection in Porous Media, Springer, Berlin, 1999.
[56] P. Forchheimer, Wasserbewegung durch boden, Z. Ver. Deutsch. Ing. 45 (1901) 1782–1788.
[57] C. Mei, J. Auriault, The effect of weak inertia on flow through a porous medium, J. Fluid Mech. 222 (1991) 647–663.
[58] M. Firdaouss, J. Guermond, Sur l'homogénéisation des equations de Navier–Stokes à faible nombre de reynolds, Comptes Rendus de l'Académie des Sciences 320 (Série I) (1995) 245–251.
[59] S. Hassanizadeh, W. Gray, High velocity flow in porous media, Transport Porous Media 2 (1987) 521–531.
[60] H. Ma, D. Ruth, The microscopic analysis of high Forchheimer number flow in porous media, Transport Porous Media 13 (1993) 139–160.
[61] J.A. Ochoa-Tapia, S. Whitaker, Momentum transfer at the boundary between a porous medium and a homogeneous fluid: I theoretical development, Int. J. Heat Mass Transfer 38 (1995) 2635–2646.
[62] J. Ni, Development of a two-phase model of transport phenomena during equiaxed solidification, Ph.D. Thesis, University of Iowa, 1991.
[63] R. Wright, Core melt progression status of current understanding and principal uncertainties, in: J. Rogers (Ed.), Heat and Mass Transfer in Severe Nuclear Reactor Accidents, Begell House, New York, 1996.
[64] M. Quintard, S. Whitaker, Transport in ordered and disordered porous media volume-averaged equations, closure problems and comparison with experiment, Chem. Eng. Sci. 48 (1993) 2537–2564.
[65] C. Marle, Ecoulements monophasiques en milieu poreux, Revue de L'Institut Francais du Pétrole XXII (10) (1967) 1471–1509.
[66] J. Wodie, T. Levy, Correction non linéaire de la loi de Darcy, Comptes Rendus de l'Académie des Sciences 312 (Série II) (1991) 157–161.